NIH Public Access
Author Manuscript
J Immunol. Author manuscript; available in PMC 2015 July 01.

Published in final edited form as:
J Immunol. 2014 July 1; 193(1): 161–169. doi:10.4049/jimmunol.1400381.

Unique Temporal and Spatial Expression Patterns of IL-33 in Ovaries during Ovulation and Estrous Cycle Are Associated with Ovarian Tissue Homeostasis

Colin I. Carlock[*], **Jean Wu**[*], **Cindy Zhou**[*,1], **Kiana Tatum**[*], **Henry P. Adams**[†], **Filemon Tan**[‡], and **Yahuan Lou**[*]

[*]Department of Diagnostic Sciences, University of Texas Health Science Center at Houston, Houston, TX 77054

[†]Department of Genetics, University of Texas M.D. Anderson Cancer Center, Houston, TX 77030

[‡]Department of Internal Medicine, University of Texas School of Medicine at Houston, Houston, TX 77030

Abstract

Ovaries are among the most active organs. Frequently occurring events such as ovulation and ovarian atresia are accompanied with tissue destruction and repairing. Critical roles of immune cells or molecules in those events have been well recognized. Interleukin 33 (IL33) is a new member of IL1 cytokine gene family. Recent studies suggest its roles beyond immune responses. We systemically examined its expression in ovaries for its potential roles in ovarian functions. During ovulation, a high level of IL33 was transiently expressed, making it the most significantly up-regulated immune genes. During estrous cycle, IL33 expression levels fluctuated along with numbers of ovarian macrophages and atresia wave. Cells with nuclear form of IL33 (nIL33$^+$ cells) were mostly endothelial cells of veins, either in the inner layer of theca of ovulating follicles during ovulation, or surrounding follicles during estrous cycle. Changes in number of nIL33$^+$ cells showed a tendency similar to that in IL33 mRNA level during estrous cycle. However, the cell number sharply dropped before a rapid increase of macrophages and surge of atresia. The drop in nIL33$^+$ cell number was coincident with detection of higher level of the cytokine form of IL33 by western blot, suggesting a release of cytokine form of IL33 before the surge of macrophage migration and atresia. However, IL33 Ab, either by passive transfer or immunization, showed a limited effect on ovulation or atresia. It raises a possibility of IL33's role in tissue homeostasis following ovarian events, instead of a direct involvement in ovarian functions.

Keywords

Cytokine; reproductive immunology; mouse; ovaries

Correspondence: Dr. Yahuan Lou, Department of Diagnostic and Biomedical Sciences, SD, The University of Texas HSC at Houston, 5326 Behavioral and Biomedical Science Building (BBSB), 1941 East Road, Houston, TX 77054, Phone: 713-486-4059, Fax: 713-486-0450, Yahuan.lou@uth.tmc.edu.
[1]Current address: Department of Cancer Biology, SD, University of Maryland, 650 W Baltimore St, Baltimore, MD 21201

NIH-PA Author Manuscript
NIH-PA Author Manuscript
NIH-PA Author Manuscript

NIH-PA Author Manuscript

NIH-PA Author Manuscript

NIH-PA Author Manuscript

Introduction

Interleukin 33 (IL33), which was discovered in 2003, is the newest member of IL1 cytokine gene family (1–3). As it was first discovered in nuclei of endothelial cells of the high endothelial venules (HEV) of lymph nodes, IL33 was originally named nuclear factor-HEV (NF-HEV)(1). Structurally, IL33 contains two domains: a histone-binding domain and an IL1-like cytokine domain (4). Thus, newly synthesized IL33 will be translocated into nucleus. Although the caspase system cleaves the protein, the generated fragment has no typical IL1 cytokine activity, which is unusual among members in this family (5). A recent study showed that cleavage of IL33 was through a different mechanism, and this cleaved fragment showed activity (6). Numerous studies have been devoted to investigating its role in immunoregulation. Those results demonstrated a regulatory role in innate immunity, as well as in Th2 T cell response, with ST2 as its receptor (7–10). More recently, IL33 has been shown to play a role as an alarmin during viral infection (11). It has been reported that the cytokine form of IL33 may be released from necrotic cells to induce immune response, and acts as a “danger signal” (12). On the other hand, mounting evidence has suggested its role beyond immune responses (13). For example, its expression has been detected widely in many human and mouse tissues (14, 15). However, it remains unclear what the role of widely expressing IL33 is, and whether it plays a role in physiological processes.

Ovaries are among the most active organs with frequent occurrence of physiological events such as ovulation, ovarian atresia and luteolysis (16). All these events are accompanied with tissue destruction and massive cell death. Multiple events such as ovulation have been reported to resemble inflammatory response (17–19). The involvement of macrophages or other leukocytes in luteinization and ovulation has been well demonstrated (20, 21). Unlike pathological inflammations, such “physiological” inflammations must be well controlled to avoid pathological consequences such as autoimmunity. Therefore, a different set of immune molecules or cells is most likely to be involved in such ovarian processes. As an essential step to understand how the immune system is involved in those physiological processes in ovaries, many studies have been devoted to examining various leukocyte subsets such as macrophages, dendritic cells and T cells, and related immune molecules such as cytokines and chemokines (22–26). Huge progresses have been made in the last decade. However, the functions of those immune cells or related molecules largely remain to be explored. In addition, the discovery of new immune molecules will surely add more dimensions for exploration.

Immune molecules, which include cytokines, chemokines, adhesion molecules and others, have been shown to play critical roles in ovarian functions (27–29). Cytokines or growth factors may be directly involved in ovarian functions such as follicle development or apoptosis (29). On the other hand, leukocyte trafficking related molecules such as chemokines and adhesion molecules recruit special immune cells during physiological processes such as ovulation (28). However, expression of these trafficking related molecules is often regulated by cytokines. Thus, investigation of ovarian expression of cytokines is especially important. Many immune molecules including cytokines have been investigated (27–31). As a newly discovered cytokine, as well as its wide expression in non-lymphoid tissues or organs, we have realized necessity of systemic examination of expression of IL33

NIH-PA Author Manuscript

NIH-PA Author Manuscript

NIH-PA Author Manuscript

in ovaries during different ovarian events. With a focus on ovulation and estrous cycle, this study has investigated its temporal and spatial expression pattern in ovaries. Our results revealed a transient high level expression of IL33 during ovulation and a unique fluctuation of IL33 expression during estrous cycle. Those observations suggest IL33's involvement in those ovarian processes.

Materials and Methods

Mice and their treatment

Balb/c females (4 to18 weeks) were purchased from Harlan (Indianapolis, IN, USA). Mice of 15–17 weeks were used for most experiments if their ages were not mentioned. The mice were maintained in the animal facility at the University of Texas Health Science Center at Houston and allowed to acclimate for a minimum of seven days. All animal procedures in this study were approved by institutional animal welfare committee. In some experiments, estrous cycle was determined in experimental mice by vaginal smear sampled at 6:00am following a published method (32). Ovaries were harvested and fixed in PFA or snap-frozen in liquid nitrogen. In some cases, ovaries were used for isolation of total RNA with a kit from Ambion (Austin TX). For induction of superovulation in mice, a previously published method was adapted (26). Briefly, the animals were injected with eCG (pregnant mare's serum gonadotropin, Sigma, St. Louis, MO) at 5 IU/mouse intraperitoneally (i.p.). After 48 hrs, the mice were injected i.p. with hCG (human chorionic gonadotropin, 5 IU/mouse, Sigma, St. Louis, MO). For injection of IL33 Ab, each mouse was injected through tail i.v. at a dose of 0.1 mg/mouse.

Abs

The following Abs were purchased from BD Biosciences (San Jose, CA): biotin labeled anti-mouse MHC class II molecules IA/IE (rat IgG2a, 2G9), Alexa-647 labeled anti-mouse CD11b/Mac-1 (M1/70), and FITC-labeled anti-mouse CD31 (clone 390). Alexa-488-labeled anti-mouse F4/80 (rat IgG2a, BM8) was obtained from Biolegend (San Diego, CA, USA). Biotinylated goat anti-mouse IL33 Ab and rat anti-mouse IL33 mAb (neutralizing)(clone 396118) were from R&D System (Minneapolis, MN) or ProSci (Charleston, SC). Another anti-IL33 mAb (Nessy-1) was from Alexis Biochemicals (San Diego, CA). FITC-labeled anti-smooth muscle α-actin (SM-α-actin) Ab (1A4) and purified anti-ZP3 (IE-10) mAb were from Sigma-Aldrich (St. Louis, MO). Secondary reagents Alexa-555, Alexa-594 and Alexa-647-labeled (Life Technologies, Carlsbad, CA) and PE labeled (BD Biosciences) streptavidin were used to visualize biotin labeled Abs. Biotin/avidin and anti-mouse CD16/32 mAb (D34-485, BD Biosciences) were used for blocking non-specific binding. Various immunoglobulin isotypes used as negative controls were from BD Biosciences.

Quantitative PCR detection of IL33 mRNA and cloning of ovarian IL33

cDNA was synthesized using 1 μg of total RNA through an RT (reverse transcription) reaction (RNA PCR Core Kit, Applied Biosystems, Foster City, CA). Conventional PCR was carried out to detect IL33 mRNA using a pair of primers ($5'$-GCTGCGTCTGTTGACACATT-$3'$, $5'$-GACTTGCAGGACAGGGAGAC-$3'$), which resulted in a 202bp product. PCR was carried out under the following conditions: pre-

NIH-PA Author Manuscript

NIH-PA Author Manuscript

NIH-PA Author Manuscript

heating at 94°C for 3 min followed by 35 cycles of PCR (94°C 1 min, 58°C 30 seconds, 72°C 1 min)(GeneAmp9700, Applied Biosystems, Foster City, CA). The products were separated by electrophoresis in 1.5% agarose gel, stained with ethidium bromide and visualized under UV light illumination. Digital images were captured by an imaging analyzer (Perkin-Elmer, Waltham, MA). Quantitative PCR (Q-PCR) was performed with a pair of primers ($5'$-CCTTCTCGCTGATTTCCAAG-$3'$ and $5'$-CCDTTACGGATATGGTGGTC-$3'$) under a similar condition as for conventional PCR using SYBR Green system (SuperArray Bioscience, Frederick, MD) on iCycler-iQ thermocycler (BioRad, Hercules, CA). Relative abundance was calculated as $2^{\Delta(t-t0)}$ with a sample as standard following a published method (30). A house-keeper gene hypoxanthine-guanine phosphoribosyltransferase (HPRT) was used as a control with a pair of primers ($5'$-CCTGCTGGATTACATTAAAGCCACTG-$3'$ and $5'$-GTCAAGGGCATATCCAACAACAAAC-$3'$).

For PCR cloning of ovarian IL33 cDNA, a high fidelity DNA polymerase (Platinum pfx, Invitrogen, Carlsbad, CA) was used with a pair of primers to cover majority of IL33 transcript ($5'$-CACCATGAGACCTAGAATGAAGTATTCCAA-3 and $5'$-TTAGATTTTCGAGAGCTTAAACATAATATT-$3'$). The PCR condition was similar to that for detection of IL33 expression but synthesis time was extended to 1 min. PCR product (800bp) of ovarian IL33 was purified on an agarose gel after electrophoresis, and directly cloned into pET101/D-TOPO vector (Invitrogen, Carlsbad, CA). Multiple independent clones of recombinant vectors were chosen and sequenced through a commercial automated DNA sequencer. The DNA sequence was compared with published mouse IL33 cDNA sequence in NCBI web.

Recombinant IL33 (rIL33) and immunization

pET101/D-TOPO vector with insert of cDNA of whole ORF of IL33 as described above was used as for expression of mouse rIL33 following our previously published method (26). The rIL33 was further purified with preparative SDS-PAGE. Briefly, the whole lysate was loaded to preparative SDS-PAGE gel. Gel was immersed into 4M sodium acetate to visualize proteins. The rIL33 bands were sliced out and rIL33 was eluted from the gel by electrophoresis. After dialyzing against PBS, the protein was lyophilized. The purity of rIL33 was checked by SDS-PAGE, and further verified by western blot using anti-rIL33 Ab. For immunization, rIL33 (5mg/ml) in PBS was mixed with CFA at 1:1. Each mouse received 50μl of the mixture. Another group of mice were immunized with CFA alone. Mice were bled from tail veins at 24 and 36 days and their sera Ab to rIL33 was tittered by western blot through serial dilution. Those mice with a titer higher than 1:1600 were used for superovulation.

Immunofluorescence, TUNEL staining, and quantitation of cells on sections

Ovaries, fixed or non-fixed depending on activity of the Abs to be used, were frozen and 3 μm frozen sections were cut. Prior to staining, all sections were blocked in 3% BSA with Abs to CD16/32. For multi-color staining, Abs which were directly conjugated to a fluorescent dye, were used. If one biotin labeled Ab was used, this Ab was used for the first staining after blocking with a biotin and avidin blocking kit from Vector BioLab

NIH-PA Author Manuscript

NIH-PA Author Manuscript

NIH-PA Author Manuscript

(Philadelphia, PA, USA). Fluorescent dye-labeled streptavidin was then used as secondary reagent. The ovarian sections observed by a fluorescent microscope (Nikon 80i Eclipse, Tokyo, Japan) and digital images were captured and analyzed with NIS Elements 3.2 from Nikon. In some cases, fluorescent images were taken by a confocal microscope in M.D. Anderson Cancer Center (Houston, TX). For TUNEL staining, a kit (In Situ Cell Death Detection Kit, Fluorescein, Roche, Nutley, NJ) was used following manufacturer's instruction. For quantitation of $IL33^+$ cells and macrophages on an ovarian section, consecutive images were captured with a Nikon Instruments Eclipse 80i with motorized stage at 20x10. Images were then combined to obtain a single super-image of the entire section with resolution at x200. Thus, each positive cell was accurately identified, marked and countered. The results for cell density was calculated by (total cells on a section)÷(total area of the same section).

Western blot

Ovaries were harvested and immediately homogenized on ice in an extraction buffer containing a protease inhibitors cocktail (Sigma-Aldrich, St Louis, MO). After centrifugation at 10,000*g* for 15 min at 4°C, the supernatant was carefully removed and its protein concentration measured. The ovarian extracts were mixed 1:1 with SDS sample buffer. Ten μg of proteins were loaded on a 12.5% SDS-PAGE and ran at a constant current. After transfer, the membrane (Immobilon-P PVDF, Millipore, Billerica, MA) was first incubated with biotin-labeled anti-IL33 Ab followed by incubation with IRDye®800CW labeled streptavidin (LI-COR, Lincoln, NE). The membrane was scanned on an infrared fluorescence scanner (Odyssey, LI-COR).

Detection of genome wide gene expression in ovaries

Three hundred ng of Total RNA were amplified and purified using Illumina TotalPrep RNA Amplification Kit (Illumina, San Diego, CA) following kit instructions. RNase H and DNA polymerase master mix were immediately added into the reaction mix following reverse transcription and were incubated for 2 hours at 16 °C to synthesize second strand cDNA. *In vitro* transcription was performed and biotinylated cRNA was synthesized by 14-hour amplification with dNTP mix containing biotin-dUTP and T7 RNA polymerase. Amplified cRNA was subsequently purified and concentration was measured by NanoDrop ND-1000 Spectrophotometer (NanoDrop Technologies, Wilmington, DE). An aliquot of 750 ng of amplified products were loaded onto Illumina Sentrix Beadchip Array Mouse Ref8_v2 arrays, hybridized at 58°C in an Illumina Hybridization Oven (Illumina) for 17 hours, washed and incubated with straptavidin-Cy3 to detect biotin-labeled cRNA on the arrays. Arrays were dried and scanned with BeadArray Reader (Illumina). Data were analyzed using GenomeStudio software (Illumina). Clustering and pathway analysis were performed with GenomeStudio and Ingenuity Pathway Analysis (Ingenuity Systems, Redwood City, CA) softwares respectively.

Statistics

T-tests (comparison between two groups) and Kruskal-Wallis with Dunn's post test (more than 3 groups) were used. Statistical significances were indicated by *($p<0.05$) or

NIH-PA Author Manuscript

NIH-PA Author Manuscript

NIH-PA Author Manuscript

**($p<0.01$). Linear regression test was used for analysis of correlation between ages and IL33 expression.

Results

A transient high level of ovarian IL33 expression during hCG induced superovulation

Two batches of total RNA from ovaries sampled at 0, 3, 6, 9 and 13 hrs (immediately after ovulation) post hCG injection from two independent experiments were used for DNA microarray for their global gene expression profiles. In both cases, gene expression pattern analysis showed that the samples from different time points formed distinct clusters, suggesting reliability of those samples (Fig. 1A and B). Ranking by significance in up-regulation of expression as compared to 0 hr shows that IL33 was the 11^{th} ($p=3.01x10^{-6}$) and 15^{th} ($p=3.72x10^{-6}$) greatest for all genes at 6hr post hCG injection for two sample batches respectively. In both cases, IL33 was ranked the first for all genes related to the immune system including cytokines, chemokine, adhesion molecules, leukocyte markers or other related molecules (Table 1). However, its significance rank rapidly dropped to 438^{th} at 9hr, suggesting very transient expression. Interestingly, gene for ST2, a known IL33 receptor, was also among top up-regulated genes related to the immune system (9^{th}) at 6hr (Table 1). Q-PCR was performed to determine IL33's mRNA levels during ovulation in detail. IL33 expression was gradually up-regulated from 0 to 3hr (Fig. 1C). A sharp increase in its expression level was followed and reached the peak at 5hr. At the peak, IL33 mRNA level was more than 170-fold greater that at 0hr. Expression levels rapid decreased from 5 to 9hr. Thus, Q-PCR also revealed a transient high level expression of IL33 in the ovaries during a narrow 6 hr window (i.e. 3 to 9hr post injection). By comparison, expression levels of the house keeper gene HPRT in ovaries nearly did not change during entire ovulatory process (Fig. 1C).

We next examined ovarian IL33 during ovulation at the protein level. Western blots detected two forms of ovarian IL33, i.e. the 30kD nuclear form and 20kD cleaved cytokine form (Fig. 1D). The nuclear form of IL33 at 6hr was more prevalent at 6 hr than any other time points, which matched the IL33 mRNA peak at 5hr. However, the cleaved form of IL33 was most abundant at 9hr when IL33 mRNA had already dropped to a low level, suggesting that the cytokine activity of IL33 was directly controlled by cleavage and release rather than at a transcriptional level. Immunofluorescence was performed to identify IL33 expressing cells. This detection was based on the nuclear form of IL33. Thus, those cells were designated as nuclear $IL33^+$ ($nIL33^+$) cells. During ovulation, $nIL33^+$ cells were present at two tissue locations. First, many $nIL33^+$ cells were found in the interstitial tissues. During the ovulatory process (i.e. 0 to 13hrs), no significant difference was observed based on semi-quantitative estimation. Late experiments showed their presence during non-ovulatory period as well, and thus, their presence was not related to ovulatory process. This group of $nIL33^+$ cells will be discussed in detail later. Second group of $nIL33^+$ cells were highly related to ovulatory processes. These $nIL33^+$ cells were only found in ovulating Graafian follicles in a high frequency at 6 hr (Fig. 2A). The majority of them were located in the inner layer of theca, and occasionally in the interface between theca and granulosa. Two-color staining revealed that nearly 60% of $nIL33^+$ cells were associated with smooth muscle α-

NIH-PA Author Manuscript

NIH-PA Author Manuscript

NIH-PA Author Manuscript

actin (SM α-actin) or CD31 expressing cells (Fig. 2B and C). Thus, nIL33$^+$ cells were most likely endothelial cells in the inner theca layer of ovulating follicles. A rapid reduction in nIL33$^+$ cell number at 9hr was observed. Interestingly, a few cells with cytoplasmic IL33 were observed. Together with western blot analysis, the reduction in nIL33$^+$ cell number suggested cleavage of nIL33 and further release of the cytokine domain of IL33 at 9hr. As an internal control, nIL33$^+$ cells were never found in the theca of any other follicles, including antral follicles in non-ovulating ovaries. A small number of nIL33$^+$ cells (about less than 30%) were also found to be located in the peripheral of granulosa layer of ovulating follicles at 9 hr, a clear distance away from the theca layer (Fig. 2D). Based on the shape of the nuclei, those cells were easily identified to be non-granulosa cells. However, they did not expression CD31 or SM α-actin, or several leukocyte markers. Their identity will need more investigation.

We next cloned ovarian IL33 to further verify its expression. RNA from ovaries harvested at 6 hrs post hCG injection was used for the cloning. PCR cloning of IL33 cDNA was performed. Eight clones from two independent RT-PCRs on two individual mice were submitted for DNA sequencing. Only a single nucleotide mutation was found from G to C, which resulted in a conservative substitution of valine with leucine at a.a. 179. No other mutations were found. Thus, cloning and sequencing verified reliability of our PCR detection of IL33 expression.

Ovarian IL33 expression is not correlated with age

Since we found a group of nIL33$^+$ cells in non-ovulating follicles, we investigated the expression pattern of IL33 in non-ovulating ovaries. IL33 mRNA was detected in ovaries as young as 4 days by RT-PCR. Its expression in ovaries was compared to those from other organs at 1 wk of age (Fig. 3A). Ovaries of 1wk already showed a constant high level of IL33 expression along with two other organs, the kidneys and lungs. Kidneys showed the highest level of IL33 mRNA, and ovaries the second highest. IL33 expression has been reported in the lung in association with allergy (11). However, ovarian IL33 expression level was higher than that in lung. More than 90% of ovaries randomly sampled after 3 wks also showed significant levels of IL33 expression. However, the expression levels were irregular and did not show a correlation with aging (Fig. 3B). Irregularity in IL33 expression level, which was well reflected by a wide range of relative mRNA abundances, suggested a potential correlation with certain ovarian functional processes or events. This prompted us to investigate its expression during the estrous cycle.

Ovarian IL33 expression level fluctuates during the estrous cycle

Female mice were monitored for their estrous cycle by vaginal smear. Three to six mice were used for each stage. Their ovaries were used for analyzing their IL33 gene expression, the number of nIL33$^+$ cells and these cells' distribution. First, quantitative PCR demonstrated a fluctuation of ovarian il33 expression levels. Its expression levels peaked at diestrus, which had a relatively large deviation, and were the lowest at estrus (Dunn's post test, estrus vs mestrus $p<0.05$ and estrus vs diestrus $p<0.01$, Fig. 4A). We next investigated the quantity of nIL33$^+$ cells and their tissue locations. In order to accurately describe the distribution pattern of nIL33$^+$ cells in the ovaries, immunofluorescent micrographs at x200

NIH-PA Author Manuscript

NIH-PA Author Manuscript

NIH-PA Author Manuscript

covering a whole ovarian section were merged to form a super-micrograph to identify each nIL33$^+$ cell (marked as a pink dot) and its location (Fig. 4B). In contrast to during ovulation, nIL33$^+$ cells were located in the interstitial tissues during non-ovulatory phases, but never in any follicles (Fig. 4D). Morphological examination suggested these cells to be endothelial cells of the vein system surrounding developing follicles or in the interstitial tissue (Fig. 4D). Two-color immunofluorescence confirmed that nIL33$^+$ cells were mostly endothelial cells, as around 70% of those cells expressed CD31 (Fig. 4E). nIL33$^+$ endothelial cells, which surrounded a developing follicle, did not distribute evenly around the follicle. A cell density gradient was observed, with most at the interior facing towards medulla, and the least facing towards ovarian surface (Fig. 4B). Some nIL33$^+$ cells were also found in corpus lutea. Density of nIL33$^+$ cells were calculated on each section. A fluctuation of nIL33$^+$ cell densities during the estrous cycle was also observed (Fig. 4A). nIL33$^+$ cells gradually increased their numbers with a tendency similar to IL33 mRNA levels from estrus to diestrus. Unlike IL33 mRNA levels, which rapid descended after diestrus, the nIL33$^+$ cell number continued to increase until proestrus. A dramatic drop in their numbers to the lowest level was observed between proestrus and estrus (estrus vs proestrus $p<0.01$, Fig. 4A). Estrus had the lowest nIL33$^+$ cell density among all stages. However, there were no significant differences among those at metestrus, diaestrus and proestrus (Fig. 4A). As the volume of an ovary may significantly change during the estrous cycle due to follicular development and luteinization, calculation of cell densities may be affected. However, absolute nIL33$^+$ cell number was again much lower at estrus than other stages. Sudden reduction in nIL33$^+$ cell number suggested a release of cytokine form of IL33. Western blot of ovarian extracts showed that the cleaved form of IL33 was detected at a much higher level at estrus than that at metestrus (Fig. 4C), despite of lowest number of nIL33$^+$ cells at estrus. Like the situation at 9hr post hCG injection, endothelial cells with cytoplasmic IL33 were frequently found (Fig. 4F). On the other hand, cells with cytoplasmic IL33 were rarely present at other stages (Fig. 4G).

Relationship between IL33 expression and ovarian macrophages or atresia

Since IL33 is a cytokine, we investigated its relationship with ovarian macrophages. There are at least 5 macrophage subsets in the ovaries (25). Using two markers (F4/80$^+$ or IA$^+$ or both), total macrophage number was calculated for each individual at each stage (n=3) (Fig. 5A). Total ovarian macrophages rapidly increased after estrus and reached the peak at metestrus ($p<0.05$, Fig. 5A). A slight but non-significant reduction in their number was observed. Macrophage numbers drop between proestrus and estrus. However, the drop was not statistically significant (Fig. 5A). A similar tendency was observed for IA$^+$ macrophages. Unlike those for total macrophages, only a few, if any, of IA$^+$ macrophages were present in the ovaries at estrus. Thus, estrus had significantly lower number of IA$^+$ macrophages than other stages (for proestrus vs estrus $p<0.05$, for estrus vs metestrus $p<0.01$, Fig. 5A).

Atresia is an important ovarian process to eliminate no-longer needed follicles during the estrous cycle. This process will ensure enough high quality follicle can mature to be ovulated. We next investigated a potential relationship between IL33 expression and ovarian atresia with a focus on developing follicles (referred as follicles from now on). Atretic

NIH-PA Author Manuscript

NIH-PA Author Manuscript

NIH-PA Author Manuscript

follicles were classified into initial, early, mid, late and obsolete stage using combination of TUNEL, anti-ZP3 antibody and IA antibodies as well as morphology (Fig. 5C to G). Initial stage was characterized by the presence of apoptotic granulosa cells with normal follicular morphology and zona pellucida (ZP) (Fig. 5D). Follicles at early atretic stage were similar to initial ones, except for the presence of invading IA^+ macrophages; the invasion was usually polarized (Fig. 5E). Follicles at mid stage displayed a recognizable but deformed follicular structure with a shrunken ZP (Fig. 5F). The most characteristic feature was absence of apoptotic cells (or only a few), aside from that, the majority of follicular cells still remained relatively "normal" (Fig. 5F). At this stage, autofluorecent granules were often present, and many $CD68^+$ macrophages were found surrounding autofluorescence, with some in their cytoplasm (Fig. 5H). At late atresia, both follicles and ZP collapsed with few cells surrounding ZP; IA^+ macrophages seemed to adhered to ZP, and no more autofluorescence was seen (Fig. 5G). In obsolete atretic follicles, only collapsed ZP was seen without any macrophages or cells (Fig. 5G). Figure 5B summarizes relative frequency of each stage of atretic follicles at each estrous phase. Atretic follicles of initial stage were often observed at estrus or metestrus, but were relatively rare for other two stages. Atretic follicles at early stage with IA^+ macrophages were most often present in diestrus and less in metestrus. Follicles of both mid and late stage were fewest, and were observed in diestrus, and sometime in metestrus. Obsolete atretic follicles were observed at all four stages. Autofluorescence reached the peak during diestrus with a large deviation and then fell sharply. As autofluoresence was most often detected at late early and mid stage of atresia, this result suggested an accumulation of atretic follicles at metestrus and diestrus. In summary, these data suggested a surge of initiation of atresia at estrus, and a cleanup of atretic follicles at proestrus, although atresia may be initiated at metestrus and diestrus. Therefore, the drop in $nIL33^+$ cell number between proestrus and estrus occurred prior to initiation of atresia surge at estrus, as well as prior to the wave of macrophages' invasion into ovaries at metestrus.

IL33 antibody or immunization with rIL33 has limited effect on ovulation

A transient high level expression of IL33 during ovulation suggested its role in ovulation. We investigated whether IL33 antibody could interfere with ovulation. A neutralizing antibody was i.v. injected into BALB/c female mice, which have previously received eCG, at −3 hr of hCG injection. As controls, mice of the same ages were injected with normal IgG. Ovulated eggs were harvested and their numbers were compared. IL33 antibody treated mice showed a slightly reduced egg number than those of control (Fig. 6A). However, the difference was not insignificant. We conducted another experiment except the time for IL33 antibody injection delayed to 0 hr post hCG injection. A marginal significance (p=0.041) was observed; IL33 antibody group showed a slightly lower numbers of eggs (Fig. 6B). To confirm if IL33 antibody was present in experimental mice, their sera post experiments were used for ELISA to measure rat IgG. All mice showed presence of rat IgG. We next immunized mice with rIL33 at 8 wks of age. Another group of mice were immunized with CFA as a control. Serum anti-rIL33 Ab was measured by western blot at 12–14 wks, and only those with a high titer (>1:1200) were selected for hCG-induced superovulation. Although a more significant reduction in ovulated eggs was observed (Fig. 6C), immunization with rIL33 Ab failed to block ovulation. In addition, no significant changes in

NIH-PA Author Manuscript

NIH-PA Author Manuscript

NIH-PA Author Manuscript

the ovaries of immunized mice were found by H-E staining. We concluded that IL33, at least its cytokine form, may not be directly involved in ovulation or atresia.

Discussion

The present study has systemically investigated IL33 expression pattern in mouse ovaries. Ovarian IL33 expression was highly significant and unique, which are supported by the following results. *First*, IL33 expression levels highly correlated with or fluctuated during special ovarian processes such as ovulation and estrous cycle. Many cytokines and chemokines have been studied for their roles in ovarian events by studying their expression during those events (16, 26–31, 33). Among all those molecules, IL33 probably is that most significantly correlated or up-regulated during a special ovarian event such as estrous cycle and ovulation. It worthwhile to remind that IL33 was the most significantly up-regulated immune molecule during ovulation. *Second*, level of IL33 expression was not neglectable. Many randomly sampled ovaries expressed a higher level of IL33 than many other organs apart from those ovaries sampled at IL33 expression peak in estrous cycle and during ovulation. Both intensity of fluorescence in microarray or quantitative PCR analysis on IL33 expression suggested its expression to be at least at mid range for all genes. At its expression peak, PCR showed that level for ovarian IL33 was close to that of a house keeper HPRT. If taking IL33 cytokine nature under consideration, it was a relatively high level of expression. Furthermore, both forms of IL33 were detectable by western blot in whole ovarian lysate. *Third*, we have identified distinct tissue location and cell type for IL33 expression. Those locations were also closely associated with special ovarian processes. For example, IL33 was expressed in inner layer of theca of ovulating follicles during ovulation, while it was mainly expressed in veins which surrounded follicles during estrous cycle. Multiple studies have reported expression of IL33 in endothelial cells (1, 34). We also showed that those IL33 expressing cells were endothelial cells.

What is the function of significantly expressed ovarian IL33? It is well known that IL33 plays regulatory roles in promoting innate immunity or Th2-related T cell response (7, 8). However, recent studies have further suggested that IL33 may also play roles beyond those immunofunctions (3, 11–15). Mounting evidence supports that IL33 may be involved in a tissue “guarding” system during both traumas and infections (11–13). As a “guarding member”, it is possible that ovarian IL33 may simply function as a part of first line of defense, just as in other organs/tissues. However it is highly questionable because of IL33’s unique expression pattern during ovarian events. Although the present study did not provide direct evidence supporting any role of IL33 in ovarian functions, our results do suggest several potential functions of IL33 in ovaries, which may or may not be related to the “guarding” system. *First*, a sharp transient expression of IL33 during 3 to 9 hrs post hCG injection and IL33’s expression location in ovulating follicles strongly suggested its role in ovulation-related inflammation. Detection of the cytokine form of IL33 at 9 hr was coincident with a drop in $nIL33^{+}$ cells, indicating a sudden release of the IL33 cytokine form. Thus, although transcription and translation of IL33 were initiated at hCG injection, the cytokine domain was released at 9 hr, just prior to initiation of inflammation-like ovulatory processes. If we ignore its function as a nuclear binding protein, IL33 could fit well into the whole picture of ovulation-related inflammation. However, our efforts to block

NIH-PA Author Manuscript

NIH-PA Author Manuscript

NIH-PA Author Manuscript

ovulation using a neutralizing antibody failed. Although our experiment did not address if the nuclear form of IL33 played any role in ovulation, a new study has demonstrated that deletion of the IL33 gene does not significantly affect female reproduction (7, private communication with Dr. Nakae). Thus, more investigations are needed to answer the question why IL33 undergoes a high level of transient expression during ovulation. Interestingly, expression of IL33 and its receptor ST2 has been detected in multiple organs including reproductive organs such as uteri (35). Their expression is detectable under physiological conditions, suggesting their potential roles in the physiological function of an organ. For example, abnormal IL-33/ST2 activation in decidualizing stromal cells prolongs uterine receptivity in women with recurrent pregnancy loss (35). On the other hand, ovarian steroids may regulate expression of IL33 (36). This again suggests that IL33 plays a role, either directly or indirectly, in reproduction. We will surely examine if ovarian IL33 expression is regulated by certain hormones.

Second, fluctuation of IL33 expression levels during the estrous cycle also suggests its potential roles in the cycle. However, unlike the ovulatory process, multiple ovarian events such as follicle development and ovarian atresia occur simultaneously or overlap each other during the estrous cycle. Therefore, it is nearly impossible to separately examine each individual process, because of complicated interaction among many types of cells and their relationship to other ovarian events. Due to this complicated situation, as well as its cytokine nature, our study first aimed to seek out the relationship between IL33 expression and ovarian immune cells especially macrophages. We then could relate the immune cells to an ovarian process, in which the immune cells are known to participate. We focused on ovarian macrophages based on the following reasons. First, numerous studies have demonstrated that macrophages play critical roles in ovarian events ranging from follicle development to luteinization (37). Secondly, multiple subsets of macrophages in ovaries have been well described by our group (25). Those macrophage subsets display distinct tissue distribution patterns, suggesting their special roles. For example, IA^+ macrophages, which express high level of MHC class II molecule (IA or IE), are mainly found in the atretic follicles. Our result showed that the number of total and IA^+ macrophages changed during estrous cycle in a similar tendency to that of IL33 expression at mRNA levels. It needs to be pointed out that IA^+ macrophages nearly disappeared from ovaries at estrus when IL33 mRNA level and $nIL33^+$ cell number also dropped to their lowest. We further compared IL33 expression with ovarian atresia since IA^+ macrophages were mainly present in atretic follicles. With a combination of multiple methods for identification of atretic follicles, we were able to describe how atresia progressed, which allowed us to classify atretic follicles into stages. Using this classification, the relative frequency of each stage of atretic follicles was determined for each estrous stage. Unlike IL33 expression and ovarian macrophages, wave of atresia during estrous cycle were much more subtle, even based on our classified atretic follicles. It is clear, however, that initiation of atresia wave occurred at estrus, because atretic follicles at initial stage (with only apoptotic cells) were mostly found at this stage but not others. It means that the initiation of atresia at estrus was coincident with the lowest points of both IL33 expression and IA^+ macrophages. In other words, the initiation of atresia was prior to a rapid increase in IA^+ macrophages. Since the increase in IL33 mRNA is

NIH-PA Author Manuscript

NIH-PA Author Manuscript

NIH-PA Author Manuscript

parallel but not prior to migrations of IA^+ macrophage, it casts doubt on any roles of IL33 in the recruitment of IA^+ macrophage into early atretic follicles.

In order to clarify the above doubt, we further did the following analysis. Our study also showed a fluctuation of nIL33 number during the estrous cycle. Through comparison of the fluctuation pattern of $nIL33^+$ cell number during the estrus cycle to that of IL33 mRNA level, we found a significant difference in the fluctuation patterns between the two. When $nIL33^+$ cell number continued to climb to a peak at proestrus, IL33 mRNA level had already fallen. This may be explained by the time required for translation. However, the both fell to their lowest point at estrus. For IL33 mRNA, it simply means a down-regulation of transcription. A sudden drop in $nIL33^+$ cell number from peak to valley at estrus, however, suggested a rapid release of cleaved IL33. This was supported by the following results. First, a higher concentration of cleaved IL33 was detected at estrus than that at metestrus. Second, clustered endothelial cells with cytoplasmic IL33 were present, while such cells were rarely observed at other stages. Thus, release of cytokine IL33 was coincident with initiation of atrsia wave but prior to massive IA^+ macrophage invasion. Based on these relationships, we are able to propose a hypothetic cascade during atresia: 1) atresia signal triggers apoptosis in follicular cells. 2) simultaneously, $nIL33^+$ endothelial cells cleave nIL33 into cytokine IL33 and release the cytokine. 3) IA^+ macrophages invade the atretic follicles, probably under regulation of IL33. IL33 has been reported to induce angiogenesis and permeability of blood vessels (38). It is possible that IL33 facilitates or promotes invasion of IA^+ macrophages into atretic follicles.

Several critical questions remain to be addressed for this hypothetic cascade. The most important question is whether those consecutive events are merely coincidence or a cause-effect cascade. Many cytokines or immune molecules have been detected during ovarian events in the past (26–31, 33). Such coincidence had prompted investigations. However, functions for a majority of those molecules still remain obscure. Like those previous studies, there are several obstacles to be overcome for addressing the cause-effect relationship. Cytokines may have similar activities using a shared receptor unit, and a defected molecule may be compensated by others. Alternatively, multiple molecules with a similar function may be involved in a single event. The function of nuclear binding form of IL33 may play a role in endothelial cells activation as a transcriptional regulator (39). Fortunately, mice with a disrupted IL33 gene are available, which will surely facilitate our need to address this critical question. Depletion of the IL33 gene doesn't seem to significantly affect female reproduction (7). Thus, we need to carefully observe on any changes in the ovaries, and to see if a similar cytokine compensates IL33's function. Second important question is how IL33 is released. Expression of IL33 by endothelial or other type of cells has been reported. It is still unclear what the nuclear form IL33's function is, and when and how they are cleaved and released. Biochemical methods have shown that a typical IL1 cleavage pathway does not generate an active fragment, while other enzymes do (5, 6). It raises a question regarding *in vivo* cleavage of IL33. A further study on naturally cleaved IL33 protein as seen in the ovaries will be necessary to understand this molecule's function. If IL33's major function is the role of a cytokine, regulation of their release is probably more relevant to our study on its function in ovaries. Majority of studies suggested that tissue injuries or cell

NIH-PA Author Manuscript

NIH-PA Author Manuscript

NIH-PA Author Manuscript

necrosis leads to release of IL33 from the damaged host cells as a “danger” signal for immune cells such as mast cells to initiate tissue repairing or immune response (11–14). Our next question is whether the situations in ovarian events is different or mimics a “danger” signal, since the ovarian events are physiological processes with tissue destruction. Finally, it cannot be ruled out at this moment that IL33 may directly regulate atresia, as several previous studies have suggested induction of atresia by cytokines such as IL1β (40).

Acknowledgments

Confocal micrographs were taken at the Microscope Core, Department of Developmental Biology, University of Texas M. D. Anderson Cancer Center at Houston. Global gene expression detection using DNA microarray was performed at Quantitative Genomics & Microarray Service Center, University of Texas, HSC at Houston. We thank Drs. Tuan Tran for technical help and April Ross for reading manuscript.

Grant Support: This study was supported by the NIH grant R01 HD049613 (Y.H.L) and partially R01 DK077857 (Y.H.L.).

Abbreviations used in this paper

eCG	equine chorionic gonadotropin
hCG	human chorionic gonadotropin
HEV	high endothelial venules
nIL33	nuclear form IL33
SM-α-actin	smooth muscle α-actin

References

1. Baekkevold ES, Roussigné M, Yamanaka T, Johansen FE, Jahnsen FL, Amalric F, Brandtzaeg P, Erard M, Haraldsen G, Girard JP. Molecular characterization of NF-HEV, a nuclear factor preferentially expressed in human high endothelial venules. Am J Pathol. 2003; 163(1):69–79. [PubMed: 12819012]
2. Schmitz J, Owyang A, Oldham E, Song Y, Murphy E, McClanahan TK, Zurawski G, Moshrefi M, Qin J, Li X, Gorman DM, Bazan JF, Kastelein RA. IL-33, an interleukin-1-like cytokine that signals via the IL-1 receptor-related protein ST2 and induces T helper type 2-associated cytokines. Immunity. 2005; 23(5):479–490. [PubMed: 16286016]
3. Liew FY, Pitman NI, McInnes IB. Disease-associated functions of IL33: the new kid in the IL-1 family. Nat Rev Immunol. 2010; 10:103–110. [PubMed: 20081870]
4. Lingel A, Weiss TM, Niebuhr M, Pan B, Appleton BA, Wiesmann C, Bazan JF, Fairbrother WJ. Structure of IL-33 and its interaction with the ST2 and IL-1RAcP receptors--insight into heterotrimeric IL-1 signaling complexes. Structure. 2009; 17(10):1398–1410. [PubMed: 19836339]
5. Cayrol C, Girard JP. The IL-1-like cytokine IL-33 is inactivated after maturation by caspase-1. Proc Natl Acad Sci USA. 2009; 106(22):9021–9026. [PubMed: 19439663]
6. Lefrancais E, Roga S, Gautier V, Gonzalez-de-Peredo A, Monsarrat B, Girard JP, Cayrol C. IL-33 is processed into mature bioacvtive forms by neutrophil elastase and cathepsin G. Proc Natl Acad Sci USA. 2012; 109(5):1673–1678. [PubMed: 22307629]
7. Oboki K, Ohno T, Kajiwara N, Arae K, Morita H, Ishii A, Nambu A, Abe T, Kiyonari H, Matsumoto K, Sudo K, Okumura K. IL-33 is a crucial amplifier of innate rather than acquired immunity. Proc Natl Acad Sci USA. 2010; 107(43):18581–18586. [PubMed: 20937871]
8. Komai-Koma M, Xu D, Li Y, McKenzie ANJ, McInnes IB, Liew FY. IL-33 is a chemoattractant for human Th2 cells. Eur J Immunol 2007. 2007; 37:2779–2786.

NIH-PA Author Manuscript

NIH-PA Author Manuscript

NIH-PA Author Manuscript

9. Sponheim J, Pollheimer J, Olsen T, Balogh J, Hammarström C, Loos T, Kasprzycka M, Sørensen DR, Nilsen HR, Küchler AM, Vatin MH, Haraldsen G. Inflammatory bowel disease-associated interleukin-33 is. 2010
10. Borish L, Steinke JW. Interleukin-33 in asthma: how big of a role does it play? Curr Allergy Asthma Rep. 2011; 11(1):7–11. [PubMed: 20931364]
11. Bonilla WV, Fröhlich A, Senn K, Kallert S, Fernandez M, Johnson S, Kreutzfeldt M, Hegazy AN, Schrick C, Fallon PG, Klemenz R, Nakae S, Adler H, Merkler D, Löhning M, Pinschewer DD. The alarmin interleukin-33 drives protective antiviral $CD8^+$ T cell responses. Science. 2012; 335(6071):984–989. [PubMed: 22323740]
12. Enoksson M, Lyberg K, Möller-Westerberg C, Fallon PG, Nilsson G, Lunderius-Andersson C. Mast cells as sensors of cell injury through IL-33 recognition. J Immunol. 2011; 186(4):2523–2528. [PubMed: 21239713]
13. Seki K, Sanada S, Kudinova AY, Steinhauser ML, Handa V, Gannon J, Lee RT. Interleukin-33 prevents apoptosis and improves survival after experimental myocardial infarction through ST2 signaling. Circ Heart Fail. 2009; 2(6):684–691. [PubMed: 19919994]
14. Demyanets S, Kaun C, Pentz R, Krychtiuk KA, Rauscher S, Pfaffenberger S, Zuckermann A, Aliabadi A, Gröger M, Maurer G, Huber K, Wojta J. Components of the interleukin-33/ST2 system are differentially expressed and regulated in human cardiac cells and in cells of the cardiac vasculature. J Mol Cell Cardiol. 2013; 60:16–26. [PubMed: 23567618]
15. Pichery M, Mirey E, Mercier P, Lefrancais E, Dujardin A, Ortega N, Girard JP. Endogenous IL-33 is highly expressed in mouse epithelial barrier tissues, lymphoid organs, brain, embryos, and inflamed tissues: in situ analysis using a novel Il-33–LacZ gene trap reporter strain. J Immunol. 2012; 188(7):3488–3495. [PubMed: 22371395]
16. Terranova PF V, Rice M. Review: cytokine involvement in ovarian processes. Am J Reprod Immunol. 1997; 37(1):50–63. [PubMed: 9138453]
17. Richards J, Russell DL, Pchsner S, Espey LL. Ovulation: new dimensions and new regulators of inflammatory-like response. Annu Rev Physiol. 2002; 64:69–92. [PubMed: 11826264]
18. Clancy KBH, Baerwald AR, Pierson RA. Systemic inflammation is associated with ovarian follicular dynamics during the human menstrual cycle. PLoS ONE. 2013; 8(5):e64807.10.1371/journal.pone.0064807 [PubMed: 23717660]
19. Spanel-Borowski, K. Atlas of the Mammalian Ovary: Morphological Dynamics and Potential Role of Innate Immunity. Springer; 2012. Follicular atresia as a proliferative and inflammatory event; p. 23-29.
20. Fukumatsu Y, Katabuchi H, Naito M, Takeya M, Takahashi K, Okamura H. Effect of macrophages on proliferation of granulosa cells in the ovary in rats. J Reprod Fertil. 1992; 96:241–249. [PubMed: 1432955]
21. Wu R, Van der Hoek KH, Ryan NK, Norman RJ, Robker RL. Macrophage contributions to ovarian function. Hum Reprod Update. 2004; 10 (2):119–133. [PubMed: 15073142]
22. Gaytin F, Morales C, Bellido C, Aguilar E, Sanchez-Criados E. Ovarian follicle macrophages: is follicular atresia in the immature rat a macrophage-mediated event? Biol Reprod. 1998; 58:52–59. [PubMed: 9472922]
23. Brännström M, Mayrhofer G, Robertson SA. Localization of leukocyte subsets in the rat ovary during the periovulatory period. Biol Reprod. 1993; 48(2):277–286. [PubMed: 8439617]
24. Brännström M, Norman RJ. Involvement of leukocytes and cytokines in the ovulatory process and corpus luteum function. Hum Reprod. 1993; 8(10):1762–1775. [PubMed: 8300842]
25. Carlock C, Wu J, Zhou C, Ross A, Adams H, Lou Y. Ovarian phagocyte subsets and their distinct tissue distribution patterns. Reproduction. 2013; 146(4):491–500. [PubMed: 23996136]
26. Zhou C, Wu J, Borillo J, Torres L, McMahon J, Lou Y. Potential roles of a special $CD8\alpha\alpha^+$ cell population and CC chemokine thymus expressed chemokine in ovulation related inflammation. J Immunol. 2009; 182:596–603. [PubMed: 19109193]
27. Büscher U, Chen FC, Kentenich H, Schmiady H. Cytokines in the follicular fluid of stimulated and non-stimulated human ovaries; is ovulation a suppressed inflammatory reaction? Hum Reprod. 1999; 14(1):162–166. [PubMed: 10374114]

NIH-PA Author Manuscript

NIH-PA Author Manuscript

NIH-PA Author Manuscript

28. Zhou C, Borillo J, Wu J, Torres L, Lou YH. Ovarian expression of chemokines and their receptors. J Reprod Immunol. 2004; 63(1):1–9. [PubMed: 15283999]
29. Terranova PF. Potential roles of tumor necrosis factor-α in follicular development, ovulation, and the life span of the corpus luteum. Dom Anim Endocrinol. 1997; 14(1):1–15.
30. Zhou C, Wu J, Borillo J, Torres L, McMahon J, Bao Y, Lou Y-H. Transient expression of CC chemokine TECK in the ovary during ovulation: its potential role in ovulation. Am J Reprod Immunol. 2005; 53:238–248. [PubMed: 15833102]
31. Machelon V, Emilie D. Production of ovarian cytokines and their role in ovulation in the mammalian ovary. Eur Cytokine Netw. 1997; 8(2):137–143. [PubMed: 9262962]
32. Byers SL, Wiles MV, Dunn SL, Taft RA. Mouse estrous cycle identification tool and images. PloS ONE. 2012; 7(4):e35538. [PubMed: 22514749]
33. Wong KH, Negishi H, Adashi EY. Expression, hormonal regulation, and cyclic variation of chemokines in the rat ovary: key determinants of the intraovarian residence of representatives of the white blood cell series. Endocrinology. 2002; 143(3):784–791. [PubMed: 11861498]
34. Sundlisaeter E, Edelmann RJ, Hol J, Sponheim J, Küchler AM, Weiss M, Udalova IA, Midwood KS, Kasprzycka M, Haraldsen G. The alarmin IL-33 is a notch target in quiescent endothelial cells. Am J Pathol. 2012; 181(3):1099–1111. [PubMed: 22809957]
35. Salker MS, Nautiyal J, Steel JH, Webster Z, Šućurović S, Nicou M, Singh Y, Lucas ES, Murakami K, Chan YW, James S, Abdallah Y, Christian M, Croy BA, Mulac-Jericevic B, Quenby S, Brosens JJ. Disordered IL-33/ST2 activation in decidualizing stromal cells prolongs uterine receptivity in women with recurrent pregnancy loss. PLoS ONE. 2012; 7(12):e52252.10.1371/journal.pone.0052252 [PubMed: 23300625]
36. Yasuo T, Kitaya K. Effect of ovarian steroids on gene expression profile in human uterine microvascular endothelial cells. Fertil Steril. 2008; 92(2):709–721. [PubMed: 18692832]
37. Care AS, Diener KR, Jasper MJ, Brown HM, Ingman WV, Robertson SA. Macrophages regulate corpus luteum development during embryo implantation in mice. J Clin Invest. 2013; 123(8):3472–3487. [PubMed: 23867505]
38. Choi Y, Choi H, Min J, Pyun B, Maeng Y, Park H, Kim J, Kim Y, Kwon Y. Interleukin-33 induces angiogenesis and vascular permeability through ST2/TRAF6-mediated endothelial nitric oxide production. Blood. 2009; 114(14):3117–3126. [PubMed: 19661270]
39. Choi Y, Park JA, Kim J, Rho S, Park H, Kim Y, Kwon Y. Nuclear IL-33 is a transcriptional regulator of NF-κB p65 and induces endothelial cell activation. Biochem Biophys Res Commun. 2012; 421(2):305–311. [PubMed: 22708120]
40. Kaipla A, Hsueh AJW. Regulation of ovarian follicle atresia. Annu Rev Physiol. 1997; 59:349–363. [PubMed: 9074768]

NIH-PA Author Manuscript
NIH-PA Author Manuscript
NIH-PA Author Manuscript

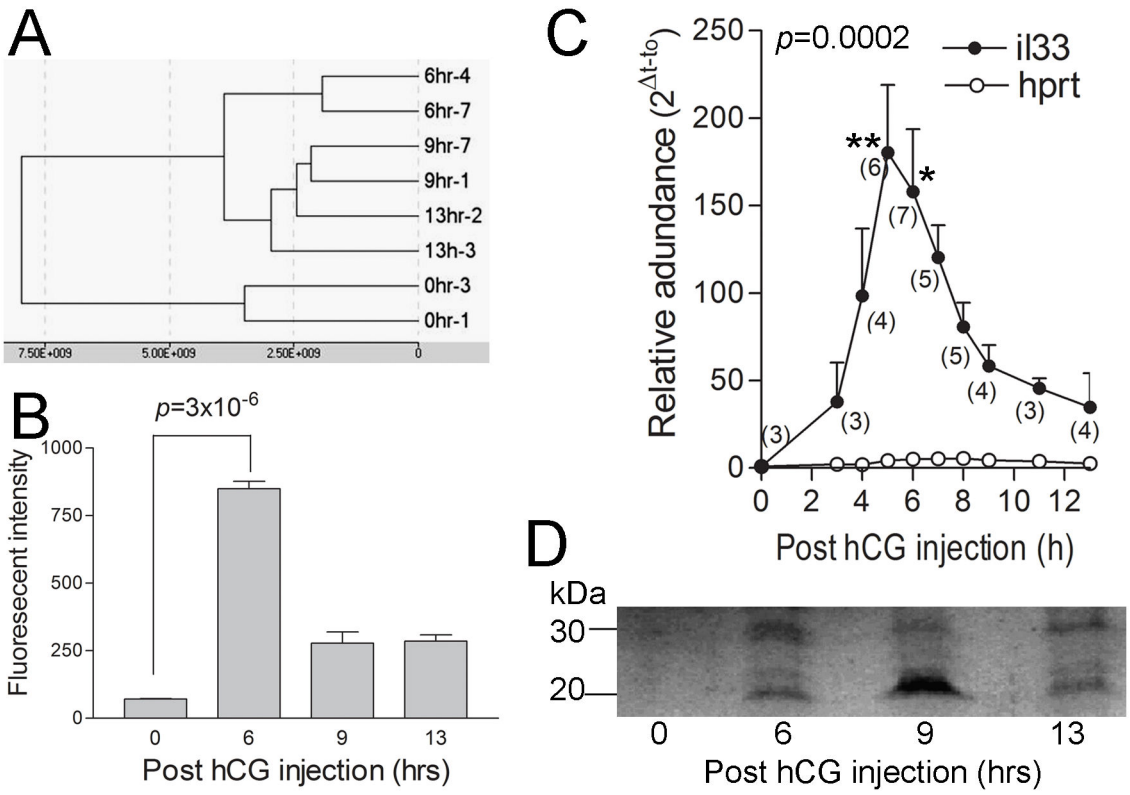

Figure 1. Ovarian IL33 expression in mice during hCG-induced ovulation

A. Clustering analysis based on global gene expression profiles from microarray shows well clustered samples from different time points post hCG-injection. Also note that the gene expression pattern for 6 hrs is significantly different from other groups. ***B.*** Microarray shows significantly up-regulated ovarian IL33 expression at 6 hrs post-hCG injection as compared to 0 hr. Expression levels were expressed as fluorescent intensity. ***C.*** Quantitative PCR detection of IL33 mRNA revealed a transient up-regulation of IL33 expression during 3 to 9 hr. A house keeper gene hprt was used as control. The number of samples at each time point is indicated in parenthesis. Kruskal-Wallis test was applied; data for each time point was compared to that for 0h with Dunn's post test. ***D.*** Western blot detection of two forms of IL33 (30kD for nuclear form and 20kD for cleaved form) at time point as indicated. Note a higher level of cytokine form of IL33 at 9 hrs. This represents similar results from 3 independent experiments.

NIH-PA Author Manuscript
NIH-PA Author Manuscript
NIH-PA Author Manuscript

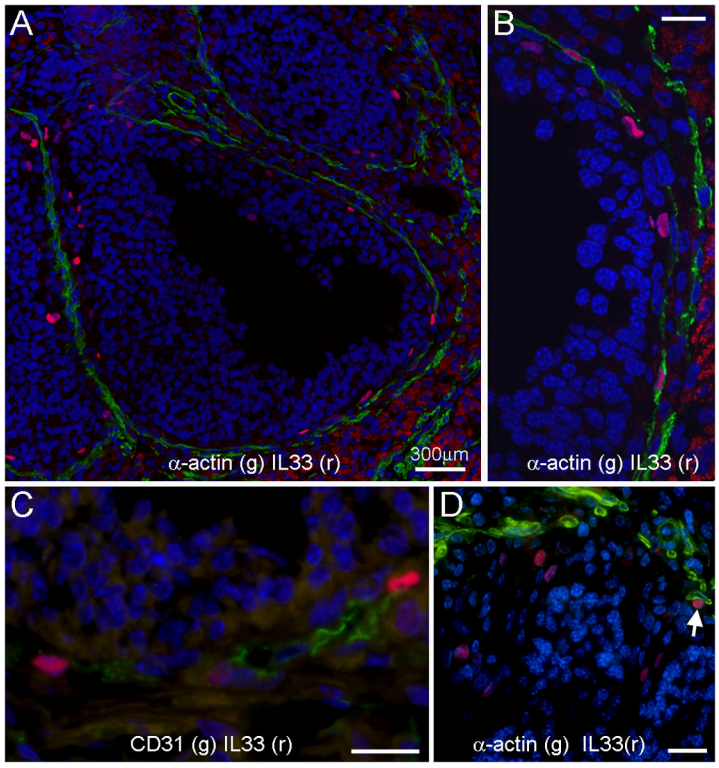

Figure 2. Tissue location of ovarian cells with nuclear IL33 (nIL33$^+$ cells) in mice during hCG-induced ovulation as detected by immunofluorescence

A. An ovulating mature follicle shows many nIL33$^+$ cells (red) around inner layer of its theca. Note that nIL33 staining (red) is colocalized to the cells, which express smooth muscle α-actin (SMα-actin, green). ***B.*** An enlarged view of co-localization of nIL33$^+$ (red) with SMα-actin$^+$ (green) cells. ***C***. nIL33$^+$ cells (red) in the theca of ovulating follicles also express CD31 (green). ***D.*** A group of nIL33$^+$ cells (red) are mingled with granulosa cells of an ovulating follicle with a distance from SMα-actin$^+$ cells (green). Note different nuclear morphology of granulosa cells and nIL33$^+$ cells. A SMα-actin associated nIL33$^+$ cell is also shown (arrow). Nuclei were counter stained by DAPI. Bars in ***B***, ***C*** and ***D*** = 20 μm.

NIH-PA Author Manuscript
NIH-PA Author Manuscript
NIH-PA Author Manuscript

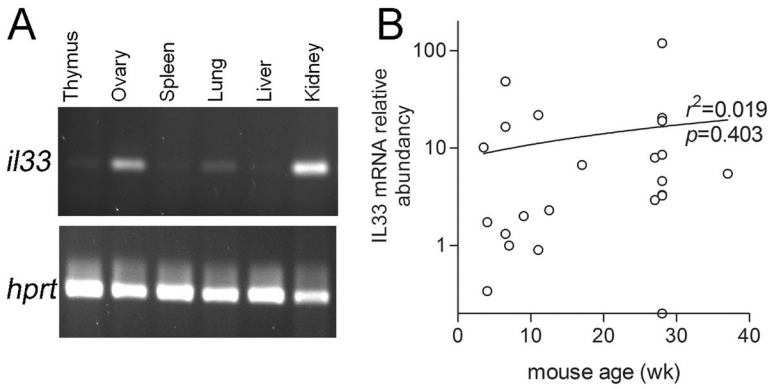

Figure 3. IL33 expression in mouse ovaries of different ages

A. A conventional RT-PCR shows IL33 expression at various organs sampled from a 1 wk old female mouse. House keeper gene HPRT was used as a control. ***B***. Quantitative PCR detection of IL33 expression in ovaries of various ages shows various but significant levels of IL33 expression in most of them. Regression analysis revealed no correlation between ages and their ovarian IL33 expression level.

NIH-PA Author Manuscript

NIH-PA Author Manuscript

NIH-PA Author Manuscript

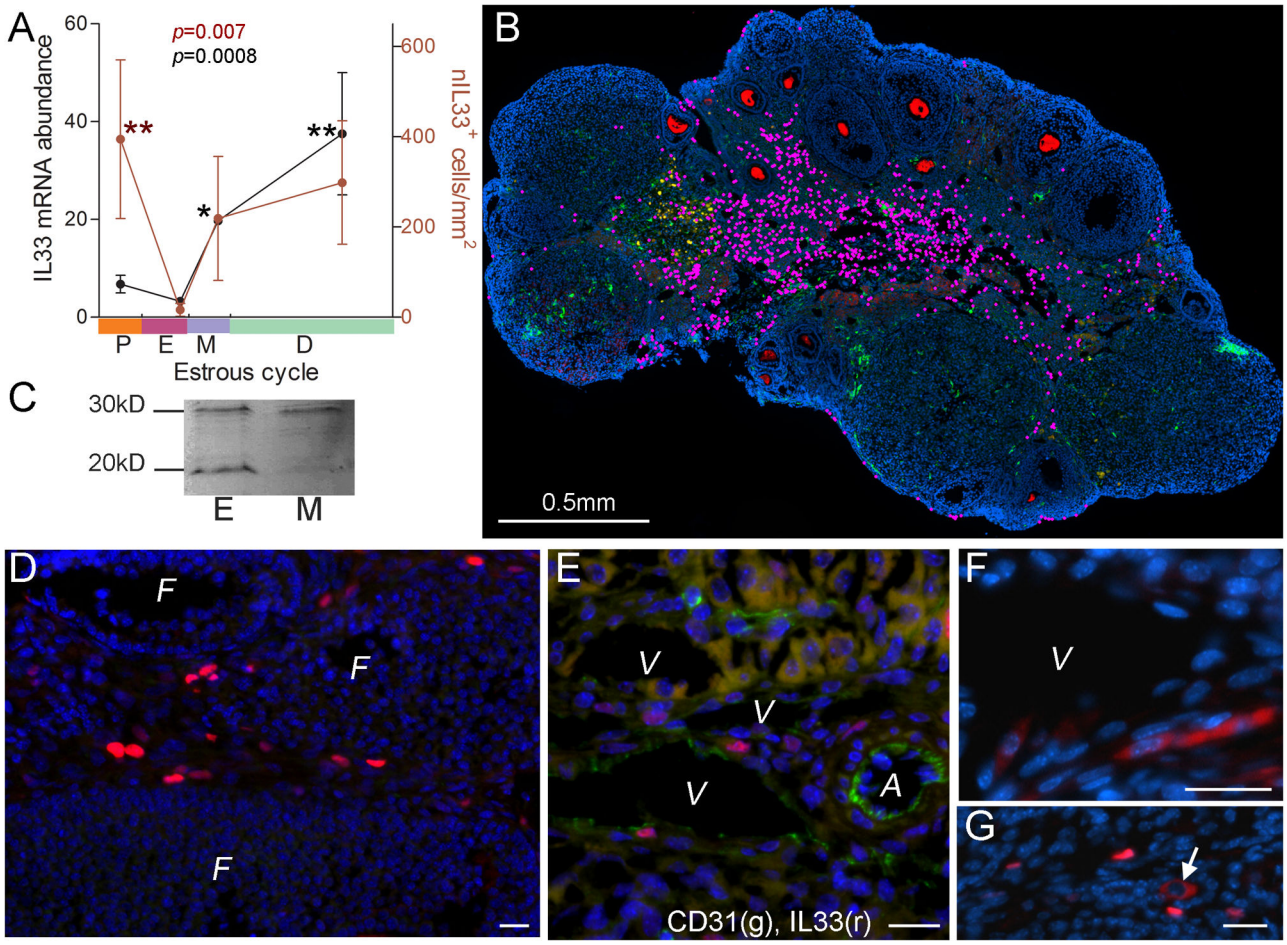

Figure 4. IL33 expression during estrous cycle in mice

A. Summary of quantitative PCR detection of IL33 mRNA (black dots and line, left y-axis) and numbers of nIL33$^+$ cells (red dots and line, right y-axis) during estrous cycle. Estrous stage in an individual was determined by vaginal smear; theoretical duration for each stage follows a published paper (32). *P*, proestrus; *E*, estrus, *M*, metestrus; *D*, diestrus. Cell numbers are expressed as cell density (cell number/mm^2). Kruskal-Wallis test was applied; data for each group was compared to that for estrus with Dunn's post test. ***B***. A representative merged super-image covering a whole ovarian section at diestrus after three-color immunofluorescence is shown. Each nIL33$^+$ cell is labeled by a pink dot for identification. Cytoplasm of oocytes is stained red. Nuclei were counter-stained by DAPI. ***C.*** Western blot detection of two forms of IL33 (30kD for nuclear form and 20kD for cleaved form) in the ovaries at estrus (E) and metestrus (M). Note a higher level of cytokine form of IL33 at estrus as compared to the lowest number of nIL33$^+$ cells during estrus cycle (***A***) at this stage. ***D***. Immunofluorescence shows a group of nIL33$^+$ cells (red) in the veins which surround various follicles (F). ***E***. Two color immunofluorescence shows nIL33$^+$ cells (red) to be CD31$^+$ endothelial cells (green); V, vein; A, artery. ***F***. A group of cells with cytoplasmic IL33 (red) are observed in endothelia of a vein (V) at estrus stage. ***G***. A cell with cytoplasmic IL33 (arrow, red) is shown to be among many nIL33$^+$ cells (red) at other stages. Bars in ***D***, ***E***, ***F*** and ***G*** = 20 μm.

NIH-PA Author Manuscript
NIH-PA Author Manuscript
NIH-PA Author Manuscript

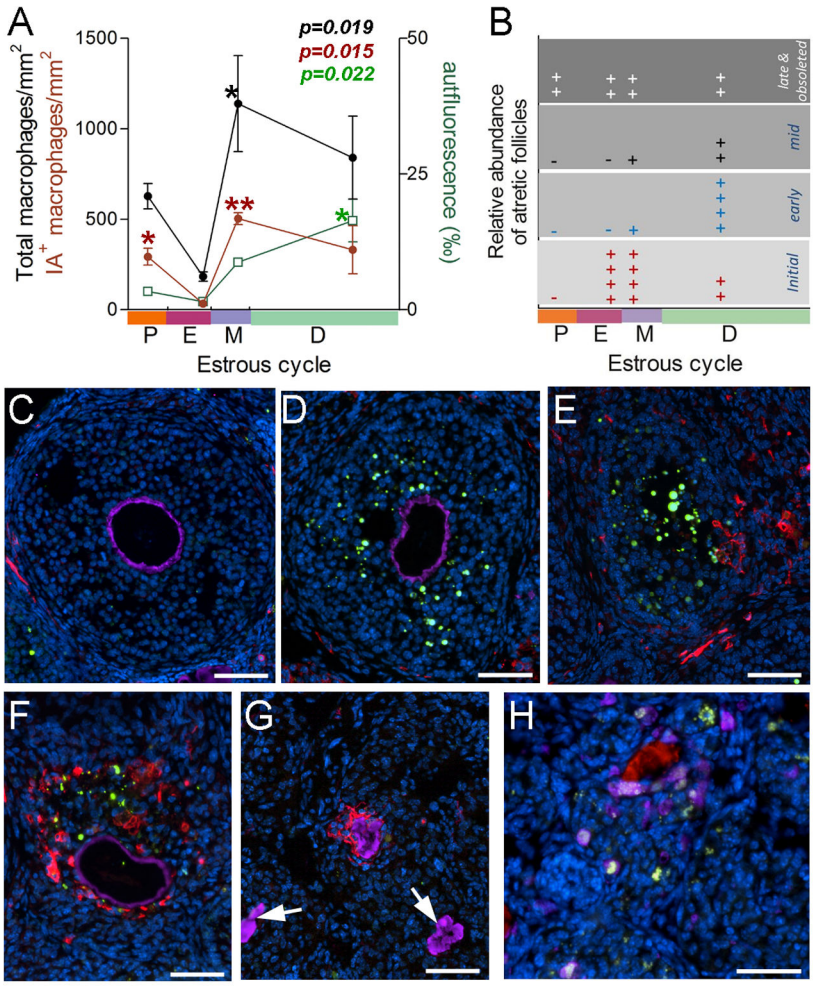

Figure 5. Variations in ovarian macrophages, atretic follicles and autofluorescence during estrus cycle in mice

A. Summary of total (black dots and line), IA$^+$ macrophages (red dot and line), or autofluorescence (green square and line) in the ovaries during the estrous cycle. Autofluorescence is expressed as ‰ of section area. Kruskal-Wallis test was applied; data for each group was compared to that for estrus with Dunn's post test. ***B***. Summary of semi-quantitative estimation of different stages of atretic follicles (see ***D*** through ***G***) at each estrous stage. ***C.*** to ***E*** are fluorescent micrographs to describe normal follicles (***C***) or atretic follicle at initial (***D***) and early (***E***) stage with four color staining: zona pellucida (purple), IA$^+$ macrophages (red), apoptotic cell (TUNEL, green) and nuclei (DAPI, blue). For staging of atretic follicles, see text; ***F*** shows an atretic follicle in a transition from early to mid with only a few apoptotic cells and many IA$^+$ macrophages; Note that the majority of follicular cells are non-apoptotic; ***G*** shows an atretic follicle at late stage with IA$^+$ macrophages. Note absence of apoptotic cells. Two obsolete follicles with remnants of zona pellucida (arrows) are also shown. ***H.*** Fluorescent micrograph shows phagocytosis of follicular cells by CD68$^+$ macrophages (purple) at mid stage. Note presence of autofluorescence in the follicles (white-green dots) and collapsed zone pellucid (red). Nuclei were counter stained by DAPI. Bars = 50 μm.

NIH-PA Author Manuscript

NIH-PA Author Manuscript

NIH-PA Author Manuscript

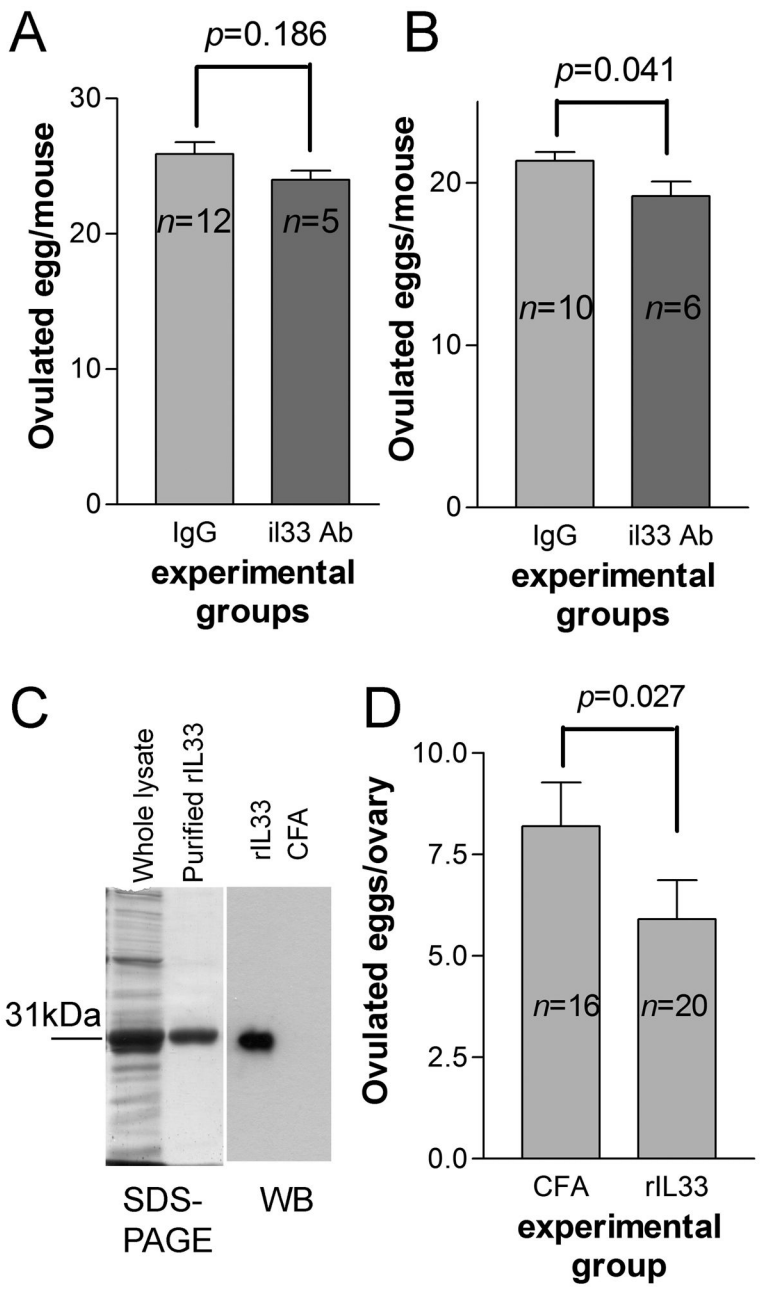

Figure 6. Interference with IL33 fails to block hCG-induced ovulation

A and ***B*** show the results of two experiments in which IL33 antibodies were injected at −6 and 0hr relative to hCG injection, respectively. The results are expressed as ovulated eggs/mouse. ***C***. the left panel shows SDS-PAGE for whole lysate and purified rIL33 as a 31kDa protein; the right panel is western blot detection of sera anti-rIL33 Ab from a representative rIL33 or CFA immunized mouse. Whole lysate was used as antigens. ***D***. Summary of hCG-induced ovulation for mice immunized with rIL33 or CFA. The results are expressed as ovulated eggs/ovary. Two-tailed unpaired *t* test was used for statistical analysis.

NIH-PA Author Manuscript

NIH-PA Author Manuscript

NIH-PA Author Manuscript

Table 1

Most significantly up-regulated genes of immune molecules during hCG induced ovulation based on genome wide DNA microarray

Gene symbol	Significance ranking	Full or other name	Basic functions
Il33	11	NF-HEV	Th2 response, alarmin
Clcf1	182	Cardiotrophin-like cytokine factor 1	IL-6 expression
Thy1	194	CD90	hematopoietic, traffic
Cd44	239		adhesion, migration
Il17r	328	IL17 receptor	Inflammation
Ccl6	411	Chemokine MRP-1	neutrophil, macrophage
Ccl7	416	Chemokine MCP-3	Macrophages
Tcrb-V8.2	488	Fragment of T cell receptor	on T cell subsets
Il1rl2	520	ST2	receptor for IL33
Cxcl14	529	Chemokine MIP-2g	monocyte, NK
Ly6c1	689		T, B cell subset marker
Ly6k	705		Unknown
Mmp19	726	Matrix metalloproteinase	Migration
Il17ra	730	Low affinity IL17 receptor	Inflammation
Cx3cl1	792	Chemokine Fractalkine	T cells, monocytes